Investigation of Coating Impact on OFDR Optical Remote Fiber-Based Sensors Performances for Their Integration in High Temperature and Radiation Environments

Serena Rizzolo, Emmanuel Marin, Adriana Morana, Aziz Boukenter, Youcef Ouerdane, Marco Cannas, Jocelyn Perisse, Sophie Bauer, Jean-Reynald Mace, Sylvain Girard

Distributed OFDR Temperature Sensors: Improvements of Their Performances in Harsh Environments

S. Rizzolo, *Student Member, IEEE*, E. Marin, A. Morana, A. Boukenter, Y. Ouerdane, M. Cannas, J. Perisse, S. Bauer, J-R. Mace and S. Girard, *Senior Member, IEEE*

***Abstract*— The response of OFDR-based temperature sensors is here investigated in harsh environments (high temperature, high radiation dose) focusing the attention on the impact of the fiber coating on the sensor performances in such environments. Our results demonstrate that the various coating types evolve differently under thermal treatment and/or radiations, resulting in a small (<5%) change in the temperature coefficient of the sensor. We identified a procedure allowing improving the sensor performances in harsh environments. This procedure consists in a pre-thermal treatment of the radiation tolerant fibers at its maximum coating operating temperature. This allows stabilizing the temperature coefficients when the fiber is exposed to the harsh constraints. Finally, we show that radiation does not affect scattering phenomenon, C_T coefficients remain identical within 1% fluctuations up to 10 MGy, and that permanent RIA reached values stands for the development of high-spatial resolved distributed temperature for harsh environment associated with high temperature (up to 300 °C) and ionizing radiation up to the MGy dose level.**

***Index Terms*— DTS, OFDR, high temperature, radiation, optical fibers.**

I. Introduction

Optical fiber sensors (OFSs) have attracted intensive research interest for several decades. They have already shown a superior advantage over their conventional electrical counterparts because of their distributed capabilities [1]. A fully distributed OFS usually operates by measuring the surrounding environment changes along the length of the sensing fiber. Several techniques have been successfully applied to fulfill this kind of measurement, such as Brillouin [2], Raman [3] [4], as well as Rayleigh scattering [5] [6]. Among a large amount of physical and chemical parameters that OFSs could measure, temperature and strain are the most widely studied [1], since many applications operating in space, military or high energy physics environments require accurate measurements of these two parameters. The integration of OFSs may be possible if these sensors resist to the combined environmental constraints such as the presence of high levels of radiation and temperature.

Our recent studies have investigated the vulnerability of Optical Frequency Domain Reflectometry (OFDR) fiber sensor to ionizing radiation [7] [8]. The study in [7] deals with the permanent γ-radiation effects up to 10 MGy on five different fibers classes, from radiation resistant to radiation sensitive ones. It is shown that the scattering mechanism at the basis of OFDR technique for the monitoring of temperature and strain is unaffected (changes within 5%), thus authorizing good precision on the distributed measurements. The investigation performed on a germanosilicate optical fiber [8] demonstrates that *in situ* distributed temperature measurements are not affected by transient radiation effects during both irradiations up to 1 MGy and recovery processes. Those results have revealed that OFDR is a powerful technique possessing an almost unaffected response by radiations opening the way to the development of new fiber-based systems in radiation environments. However, both in [9] and in [10] it is reported that distributed measurements can be affected by the sensor packaging (including coating, metallic tubes, bridles …) resulting in errors caused by an inaccurate calibration.

To investigate this packaging related error sources an accurate study on double acrylate coated fibers was carried out in [9] and [11] showing that both temperature and radiation affect the temperature sensor response influencing the calibration coefficients of the fiber under test. The results showed also that a pre-thermal treatment up to 80°C and/or a pre-irradiation up to 3 MGy reduce the coating linked error on C_T and C_ε variations from 5% to 0.5% improving the performances of fiber sensors for operation in harsh environments.

In this paper, we study the response of three pure-silica-core (PSC) radiation resistant fibers possessing different coatings permitting their employment up to 300°C. The goal here is to clarify the role of the high-temperature coatings in distributed temperature measurements to investigate the possibility to

Manuscript received December 17, 2015.
S. Rizzolo is with Univ-Lyon, Lab. Hubert Curien, CNRS UMR 5516, Saint-Etienne, France, with Dipartimento di Fisica e Chimica, Università degli Studi di Palermo, Palermo, Italy and also with Areva Centre Technique, Le Creusot, France (e-mail: serena.rizzolo@univ-st-etienne.fr)
E. Marin, A. Boukenter, Y. Ouerdane, S. Girard are with Univ-Lyon, Lab. Hubert Curien, CNRS UMR 5516, Saint-Etienne, France.
A. Morana and Jocelyn Perisse are with Areva NP, Lyon, France
M. Cannas is with Dipartimento di Fisica e Chimica, Università degli Studi di Palermo, Palermo, Italy.
Sophie Bauer is with Areva Centre Technique, Le Creusot, France
Jean-Reynald Mace is with Areva, Paris-La Défense, France

enlarge the range of application of the OFSs and improve the performances of these sensors. Thermal and radiation impacts, up to 300°C and 10 MGy respectively, are the subject of this study, in which we will present a method to overcome the observed limitations in distributed temperature measurements.

II. Materials and methods

In this work we investigated the response of three commercial single mode optical fibers (named SMF-A, SMF-B and SMF-C) in the class of radiation resistant ones. Indeed, the samples have a PSC, a depressed F-doped cladding to ensure the light guidance into the core, and different coatings. In particular, SMF-A possesses a high temperature acrylate coating (HTA, diameter of about 250 µm) able to resist up to 150 °C, SMF-B is coated with polyimide (Pl, diameter of about 150 µm) and SMF-C is surrounded firstly by a thin layer of carbon, ~20 nm, and secondly by the polyimide (Pl&C, diameter of about 150 µm). These last two fibers are designed to resist both to temperatures up to 300 °C, whereas SMF-C prevents the H_2 penetration within the fiber core.

The three fibers were γ-irradiated using the BRIGITTE ^{60}Co source of SCK-CEN (Mol, Belgium) [12]. The accumulated dose on our samples varies from 1 up to 10 MGy(SiO_2), depending on the sample position with respect to the ^{60}Co source. The dose-rate and the temperature range from 10 to 30 kGy(SiO_2)/h and from 30 to 50 °C, respectively. For each of the three fibers described above we obtained four different samples irradiated at 1, 3, 6 and 10 MGy in addition to the non-irradiated reference one.

Distributed temperature sensors performances were evaluated with the OFDR technique permitting to detect the scattering figure of the fiber along its length thanks to a Mach-Zehnder interferometer. The light from a tunable laser source is split between a reference arm and a second arm where the fiber to test is connected; the backscattered light from the sample is then recombined with that of reference arm and the interference fringes from the two orthogonal polarization states are collected. Then a Fourier transform is applied to obtain the scattering figure along the length of the sample.

To get information about temperature along the optical fibers we investigate on local modification induced when heat is applied into the samples. Indeed, an external stimulus, changing locally the physical length of the sample or the refractive index distribution, modifies the optical path of the back-propagating light that can be detected and used to achieve sensing information. So, a sensor is formed by storing the Rayleigh trace in a reference state, with well-defined environmental conditions, and then correlating it with the measurement performed when a perturbation is applied along a segment of the samples. The cross-correlation is done along small sensing segment of fiber Δx, thus defining the spatial resolution of distributed sensor. Perturbation induced changes are deduced from cross-correlation in terms of a spectral shift, $\Delta\lambda$ or $\Delta\nu$, by:

$$\frac{\Delta\lambda}{\lambda_C} = -\frac{\Delta\nu}{\nu_C} = C_T\Delta T + C_\varepsilon\varepsilon \qquad (1)$$

where λ_C and ν_C are the central wavelength and frequency; C_T and C_ε are temperature and strain calibration coefficients (typical values for Germanium-doped silica core fibers are 6.48×10^{-6} $^oC^{-1}$ and $0.780\mu\varepsilon^{-1}$ [13], [14]); ΔT and ε are the applied temperature and strain changes.

To perform our study we used an OBR 4600 from Luna Technologies which has a laser at a center wavelength, λ_C, of 1550 nm (with an accuracy of 1.5 pm) and it was tuned over a rage of 21 nm, yielding to a spatial resolution of 40 µm for the scattering pattern along a maximum fiber length of 70 m, whereas spatial resolution of distributed temperature measurement, given by the choice of Δx, was set at 1 cm.

We performed four identical thermal treatments on all samples (non-irradiated and irradiated ones) to extract the C_T and to study its permanent evolution with the number of thermal treatments; also the total ionizing deposited dose dependence of the C_T was studied. The temperature profile of the thermal treatments changes samples by samples, to reach the maximum operating temperature of each coating. A summary of experimental details is reported in Table I.

TABLE I

Samples and details for Thermal Treatments.

Fiber Name	Coating	$T_{MIN} \rightarrow T_{MAX}$	ΔT	Time profile
SMF-A	HTA	30 °C → 150 °C	10 °C	10 °C/min during the heating ramp, then 30 min step at constant temperature
SMF-B	Pl	30 °C → 300 °C	30 °C	
SMF-C	Pl&C	30 °C → 300 °C	30 °C	

The thermal treatments were performed with an oven equipped with type K thermocouples that were used as reference for the measurements. For each optical fiber, we spliced together ~ 3 m long segments of the non-irradiated and of the samples irradiated at 1, 3, 6 and 10 MGy resulting in a total sample length of ~15 m inside the oven (see Fig.1 (a)). Only the sample obtained from SMF-A was formed by segments composed of a non-coated part, obtained thanks to chemical treatment at room temperature to avoid a mechanical stress induced by stripping the fibers, placed between two coated segments. This configuration allows us to study this particular sample in its non-coated state to evaluate the real coating impact on temperature sensors.

These samples were used to measure the spectral shift of Eq. (1) when varying the oven temperature. An example of the measured traces is reported in Fig. 1 (b) where spectral shift as a function of the length for the about 15 m of SMF-A sample is given for temperature ranging from 30°C to the max operating T of 150°C for the HTA coating. By considering this set of traces, we are able for each segment, non-irradiated and irradiated at the four doses, to extract its temperature coefficient C_T. An average of the spectral shift along the segment, separating coated and non-coated parts when needed, allows estimating the coefficient and its experimental error, whereas the error on distributed temperature measurements is given from the data dispersion of spectral shift trace that is shown in Fig. 1 (c) for the measurement at 100 °C and for the 3 MGy dose. C_Ts are extracted, performing a linear fit, from the calibration curves reported in Fig. 1 (d) for SMF-A samples.

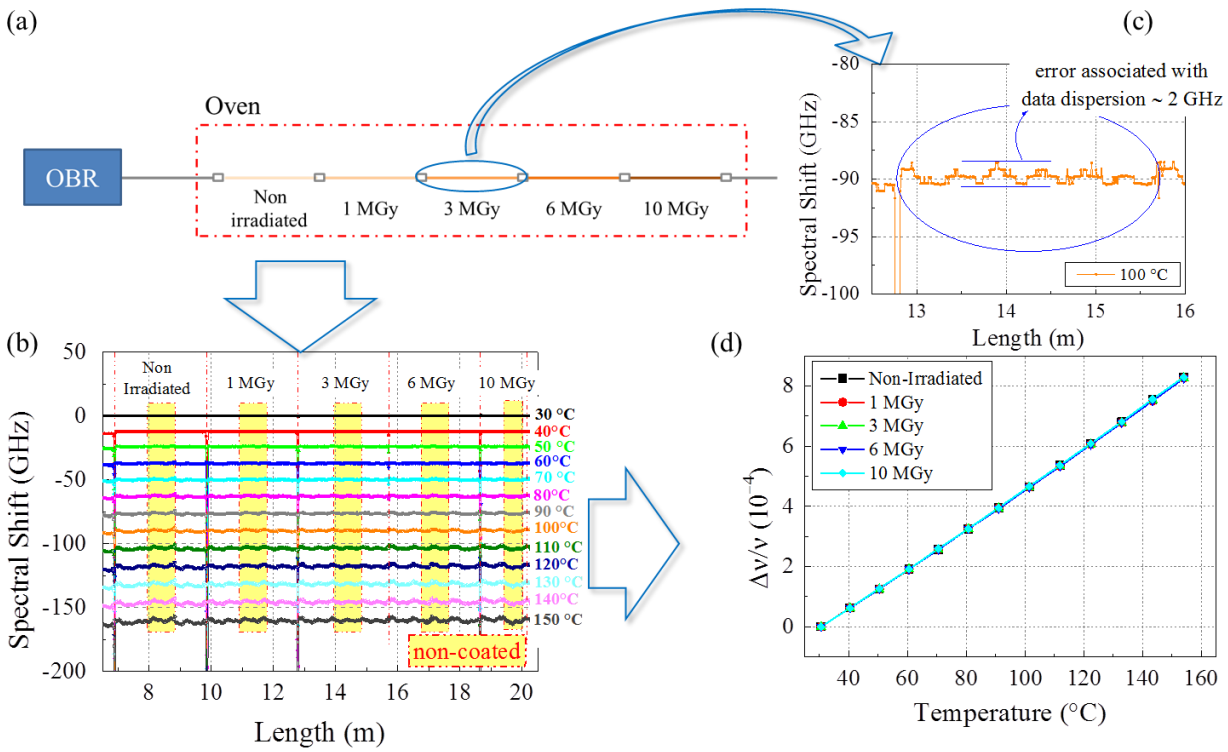

Fig. 1 (a) Schematic of temperature calibration measurements: the optical fiber path, formed by ~3 m long segments of non-irradiated and irradiated samples of the same fiber spliced to each other, is connected to OBR and placed in an oven. (b) Spectral shift as a function of the sample path length for the SMF-A at the different temperature steps during the first thermal treatment. The non-irradiated, as well as the irradiated segments at 1 MGy, 3 MGy, 6 MGy and 10 MGy are highlighted by dotted red lines. For each segment a yellow window puts in evidence the non-coated zone placed between two coated ones and obtained by chemical etching; the graph in (c) reports a zoom of the highlighted part in (a) to put in evidence the spectral shift variation along the 3 MGy irradiated SMF-A sample at 100 °C that gives the distributed measurement incertitude. Finally in (d) the calibration curves, which allow determining the temperature coefficients, are reported.

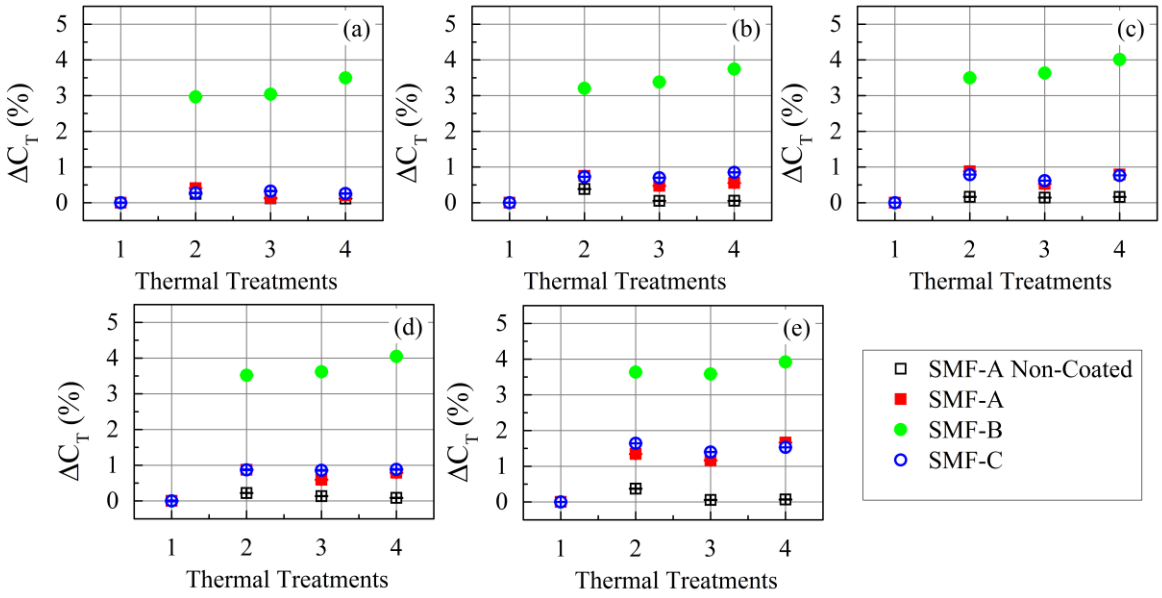

Fig. 2 Variation of temperature coefficients in consecutive thermal treatments with respect to the first one for non-coated samples (black empty squares), HTA coated fiber (red solid squares), Pl coated fiber (green solid circles) and Pl&C coated fiber (blue open circles) samples (a) non-irradiated, irradiated at (b) 1 MGy (c) 3 MGy (d) 6 MGy and (e) 10 MGy.

Finally, we investigate on permanent radiation effects through RIA measurements using ~25 m long samples irradiated at the different doses. These RIA measurements were performed with an optical time domain reflectometer (OTDR, EXFOFTB-7400E). The optical fiber attenuation was evaluated at 1550 nm with a pulse width signal of 10 ns (spatial resolution ~ 1 m) and an exposure time of 180 s.

III. Results and Discussion

Table II reports the evolution of C_Ts as a function of the four consecutive thermal treatments for the three studied optical fibers and all the considered doses of irradiation. Moreover, the SMF-A fiber in both non-irradiated and irradiated configurations has been tested twice: with and without its HTA coating. In this case, the non-coated SMF-A serves as a reference to highlight the coating's impact on the evolution of C_T with the thermal treatments. These results are shown in Fig. 2 that illustrates the variation of the C_T coefficient obtained after each of the four consecutive thermal treatments with respect to the first one.

We observe that in the case of non-coated SMF-A fiber C_T remains stable in non-irradiated and irradiated samples within 0.5%.

TABLE II

Temperature coefficients extracted from OFDR measurements and relative errors for the different coated samples.

*Thermal treatments

TT*	**C_T (10^{-6} °C^{-1})**				
	Non Irradiated	1MGy	3MGy	6MGy	10MGy
SMF-A Non-Coated					
I	6.75±0.02	6.69±0.01	6.75±0.01	6.73±0.01	6.64±0.02
II	6.76±0.02	6.72±0.01	6.76±0.01	6.75±0.01	6.67±0.02
III	6.74±0.01	6.70±0.01	6.74±0.01	6.72±0.01	6.64±0.02
IV	6.74±0.02	6.70±0.01	6.74±0.01	6.72±0.01	6.65±0.02
SMF-A High Temperature Acrylate (HTA)					
I	6.72±0.02	6.68±0.02	6.69±0.01	6.68±0.03	6.71±0.01
II	6.74±0.02	6.73±0.01	6.75±0.01	6.74±0.02	6.80±0.02
III	6.73±0.02	6.71±0.01	6.73±0.01	6.72±0.03	6.79±0.02
IV	6.73±0.02	6.72±0.02	6.74±0.01	6.73±0.03	6.82±0.03
SMF-B Polyimide (Pl)					
I	7.48±0.01	7.47±0.05	7.58±0.02	7.46±0.02	7.42±0.04
II	7.71±0.02	7.71±0.05	7.85±0.02	7.73±0.02	7.70±0.05
III	7.71±0.02	7.72±0.06	7.86±0.03	7.73±0.02	7.69±0.05
IV	7.75±0.02	7.75±0.06	7.89±0.02	7.77±0.01	7.72±0.04
SMF-C Polyimide and Carbon (Pl&C)					
I	7.87±0.04	7.82±0.02	7.84±0.01	7.83±0.09	7.77±0.01
II	7.85±0.04	7.88±0.02	7.90±0.01	7.90±0.04	7.90±0.01
III	7.84±0.04	7.87±0.02	7.88±0.01	7.89±0.04	7.88±0.01
IV	7.85±0.04	7.89±0.02	7.90±0.01	7.90±0.04	7.89±0.01

The other results show that for all coatings and for all total deposited doses the C_T coefficient increases between the first to the second thermal treatment. By considering the whole sample set, it is clear that the amplitude of these variations depends on both the fiber coating and the irradiation dose. The following thermal treatments have less impact and the C_T coefficient is stabilized (fluctuations lower that 1%). We have, in non-irradiated samples, a maximum C_T change of 3% for Pl coating, whereas variations are within the uncertainty for HTA and Pl&C coatings [Fig. 2 (a)]. For irradiated samples [see Fig. 2 (b), Fig. 2 (c), Fig. 2 (d) and Fig. 2 (e)] the C_T coefficient variation remains constant for Pl coating (3% in 1MGy and 4% in 3, 6 and 10 MGy samples), whereas it increases with the irradiation dose for HTA and Pl&C coatings up to 2% at 10 MGy.

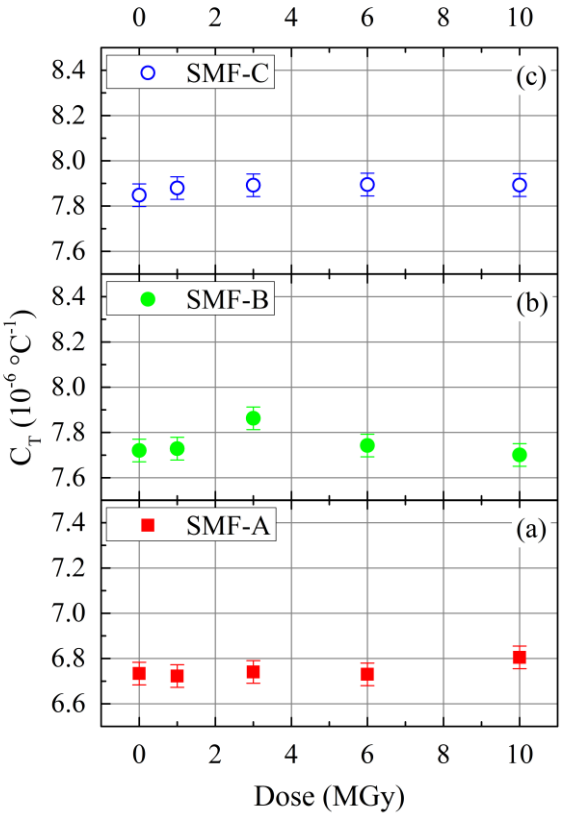

Fig. 3 Temperature coefficients as a function of total deposited dose for (a) HTA coated fiber (red solid squares), (b) Pl coated fiber (green solid circles) and (c) Pl&C coated fiber (blue open circles).

This effect, as discussed in [8] and [10] can be explained by the influence of thermal treatment on the coating which is subjected to a dilatation that releases part of the internal stress into the fiber. We can observe that for HTA, Pl and Pl&C the effect is reduced compared to the case of double acrylate coating (DAC), where C_T variations reach 5-10% between the first and the second thermal treatment [10]. Since the radiation changes the properties of coating [8], it behaves itself as a pre-thermal treatment and can stabilize the C_T coefficient. For the samples investigated in this work, this effect of radiation on coating properties is still present, even if considerably

reduced, in SMF-A and SMF-C samples. In the case of SMF-B instead we notice that the C_T variation remains constant for all the doses.

To deeply investigate the radiation effects on the different coatings, we made an average of C_T values obtained from the different thermal treatments excluding the first one, since we showed that temperature coefficient is not stable after such unique treatment. These data allow us to find the trend of C_T coefficient as a function of the total deposited dose, reported in Fig. 3 for SMF-A (a), SMF-B (b) and SMF-C (c). We observe that HTA, Pl and Pl&C coated fibers exhibit stable C_Ts as a function of radiation with variation within 1% except for the SMF-B irradiated at 3 MGy where variation is 2%. These results confirm that HTA, Pl and Pl&C are more resistant coating to both temperature and radiation constraints than DAC, for which irradiation was a factor to take in account since it introduces errors of the order of 5% in F-doped fibers [9].

The results reported in the paper, especially those of Fig. 3, suggest that radiation does not affect permanently Rayleigh mechanisms at the basis of distributed temperature sensors; calibration procedure introduced errors are indeed mostly due to the thermal stabilization of the coating achieved with a thermal treatment up to the maximum operating temperature.

TABLE III

SUMMARY OF RIA RESULTS

Fiber	RIA at 1550 nm (dB/km)			
	1 MGy	3 MGy	6 MGy	10 MGy
SMF-A	64±6	96±9	108±10	117±20
SMF-B	60±6	90±9	115±10	125±20
SMF-C	55±6	85±9	100±10	120±20

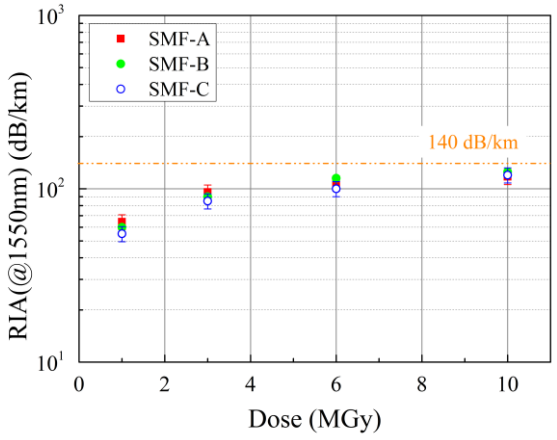

Fig. 4 Permanent radiation induced attenuation at 1550 nm after irradiation at the doses of 1 MGy, 3 MGy, 6 MGy and 10 MGy for SMF-A (red points), SMF-B (green points) and SMF-C (blue points). Orange dotted line indicates losses limitation tolerated by OFDR for a sensing range of 70 m.

It is well known, however, that radiation induces other effects degrading optical fibers properties and then sensor performances [15]. The most important being radiation induced attenuation (RIA) that affects light propagation along the fiber length. As discussed in [7] and [8], for OFDR-based distributed sensors, RIA has a strong impact on the maximum sensing length. To evaluate the response of our samples, we estimated permanent RIA by linear attenuation measurements in the irradiated samples. The results are shown in Fig. 4 for the three samples as a function of the total deposited dose. We can see that RIA has a saturation trend and it reaches similar values (summarized in Table III) at all the doses, within the experimental error; as expected, no differences are present between the different coatings. The figure highlights also the maximum value of losses tolerated by OFDR for 70 m long fiber. We see that the three fibers here studied reach permanent losses that are lower than this limit. These permanent losses are lower than the ones obtained during *in situ* measurements at the same irradiation conditions, where some unstable defects also contribute to RIA [16]. Nevertheless, it is worth to mention that the total deposited dose expected for most of applications in nuclear power plants or high energy physics facilities is largely lower than the maximum accumulated dose reached in our measurements and then our results *ex situ* remain valid.

IV. CONCLUSION

In this work we evaluated the response of three PSC single mode fibers with special coatings to be employed as distributed temperature sensors in harsh (high temperature, high dose) environments.

We investigated the impact of such special coating on OFDR-based temperature sensors performances up to 300 °C and 10 MGy respectively. We found that the temperature coefficient C_T obtained from the sensor calibration is influenced by temperature effects on coating. This influence manifests itself with a variation of C_T up to 3% between the first and the second thermal treatment, then stabilizing within fluctuation of 0.5% for the following treatments. As a consequence, a pre-thermal treatment on OFDR-based sensor up to the maximum fiber coating operating temperature is a good procedure to improve distributed temperature sensor performances before its integration in the harsh environments.

Moreover, we characterized the radiation influence on Rayleigh scattering and attenuation mechanisms. Obtained results suggest that radiation does not affect scattering phenomenon as the C_T coefficients remain unvaried within 1% fluctuations up to 10 MGy.

This information, together with the estimation of permanent RIA values in these radiation-tolerant samples allows going towards the development of high-spatial resolved distributed temperature sensors with no impact on the sensing length (up to 70 m) in presence of harsh constraints of temperature up to 300 °C and ionizing radiation up to the MGy level.

REFERENCES

[1] X. Bao and L. Chen, "Recent Progress in Distributed Fiber Optic Sensors," Sensors, vol. 12, pp. 8601-8639, 2012.

[2] X. Phéron, S. Girard, A. Boukenter, B. Brichard, S. D. Lesoille, J.

Bertrand, and Y. Ouerdane, "High γ-ray dose radiation effects on the performances of Brillouin scattering based optical fiber sensors," Opt. Express, vol. 20, no. 24, pp. 26978-26985, 2012.

[3] C. Cangialosi, Y. Ouerdane, S. Girard, A. Boukenter, S. Delepine-Lesoille, J. Bertrand, C. Marcandella, P. Paillet, M. Cannas, "Development of a Temperature Distributed Monitoring System Based on Raman Scattering in Harsh Environment," IEEE Transactions on Nuclear Science, vol. 61, no. 6, p. 3315 – 3322, 2014.

[4] C. Cangialosi, S. Girard, A. Boukenter, M. Cannas, S. Delepine-Lesoille, J. Bertrand, P. Paillet, Y. Ouerdane, "Hydrogen and radiation induced effects on performances of Raman fiber-based temperature sensors," Journal of Lightwave Technology, vol. 33, no. 12, pp. 2432 - 2438 , 2015.

[5] A. Faustov, A. Gusarov, L. B. Liokumovich, A. A. Fotiadi, M. Wuilpart, P. Mégret, "Comparison of simulated and experimental results for distributed radiation-induced absorption measurement using OFDR reflectometry," Proc. SPIE, vol. 8794, no. 87943O, 2013.

[6] A. Faustov, A. Gusarov, P. Mégret, M. Wuilpart, A. V. Zhukov, S. G. Novikov,V. V. Svetukhin, and A. A. Fotiadi, "The Use of Optical Frequency Domain Reflectometry in Remote Distributed Measurements of the γ Radiation Dose," Tech Phys Lett, vol. 41, no. 5, p. 414–417, 2015.

[7] S. Rizzolo, A. Boukenter, E. Marin, M. Cannas, J. Perisse, S. Bauer, J-R. Mace, Y. Ouerdane, S. Girard, "Vulnerability of OFDR-based distributed sensors to high γ-ray doses," Opt. Express, vol. 23, no. 15, pp. 18997-19009, 2015.

[8] S. Rizzolo, E. Marin, M. Cannas, A. Boukenter, Y. Ouerdane, J. Perisse, S. Bauer, J-R. Mace, C. Marcandella, P. Paillet and S. Girard, "Radiation Effects on OFDR based sensors," Opt. Letters, vol. 40, no. 20, pp. 4571-4574, 2015.

[9] S. Rizzolo, C. Sabatier, A. Boukenter, E. Marin, Y. Ouerdane, M. Cannas, J. Perisse, J-R. Mace, S. Bauer and S. Girard, "Radiation Vulnerability of Optical Frequency Domain Reflectometry Fiber-Based Distributed Sensors," IEEE Trans. Nucl. Sci., Submitted to, 2015.

[10] A. Faustov, "Advanced fibre optics temperature and radiation sensing in harsh environments," Ph.D. dissertation, Univ. de Mons, Mons, Belgium, 2014.

[11] S. Rizzolo, E. Marin, A. Morana, A. Boukenter, Y. Ouerdane, M. Cannas, J. Périsse, S. Bauer, J.-R. Mace, S. Girard , "Coating impact and radiation effects on optical frequency domain reflectometry fiber-based temperature sensors," in Proc. SPIE 9634, 24th International Conference on Optical Fibre Sensors, 96346U .

[12] A. Fernandez Fernandez, P. Rodeghiero, B. Brichard, F. Berghmans, A. H. Hartog, P. Hughes, K. Williams and A. P. Leach, "Radiation-tolerant Raman distributed temperature monitoring system for large nuclear infrastructures," IEEE Trans. Nucl. Sci., vol. 52, no. 6, pp. 2689-2694, 2005.

[13] B. J. Soller, D. K. Gifford, M. S. Wolfe and M. E. Froggatt, "High resolution optical frequency domain reflectometry for characterization of components and assemblies," Opt. Express, vol. 13, no. 2, pp. 666-674, 2005.

[14] B. J. Soller, M. Wolfe, M. E. Froggatt, "Polarization resolved measurement of Rayleigh backscatter in fiber-optic components," in OFC Technical Digest, Los Angeles, 2005.

[15] S. Girard, J. Kuhnhenn, A. Gusarov, B. Brichard, M. Van Uffelen, Y. Ouerdane, A. Boukenter, and C. Marcandella, "Radiation Effects on Silica-Based Optical Fibers: Recent Advances and Future Challenges," IEEE Trans. Nucl. Sci., vol. 60, no. 3, pp. 2015 - 2036, 2013.

[16] M. Van Uffelen, "Modélisation de systèmes d'acquisition et de transmission à fibres optiques destinés à fonctionner en environnement nucléaire," Ph.D. dissertation, Université de Paris XI, Paris, France,, 2001.